Maximilian Felix Wilhelm, Uwe Füssel, Thomas Richter, Matthias Riemer, Martin Foerster

Analysis of the shear-out failure mode for CFRP connections joined by forming

Erstveröffentlichung in / First published in:

Journal of Composite Materials. 2015, 49(8), S. 981 - 993 *[Zugriff am: 15.08.2019]*. SAGE journals. ISSN 1530-793X.

DOI: https://doi.org/10.1177//0021998314528264

Article

JOURNAL OF COMPOSITE MATERIALS

Journal of Composite Materials
2015, Vol. 49(8) 981–993

DOI: 10.1177/0021998314528264
jcm.sagepub.com
SAGE

Analysis of the shear-out failure mode for CFRP connections joined by forming

Maximilian Felix Wilhelm[1], Uwe Fuessel[2], Thomas Richter[1], Matthias Riemer[1] and Martin Foerster[1]

Abstract

In this paper, we look at the shear-out failure of carbon fiber reinforced plastics connections in the automotive industry. Contrary to the aircraft industry, the boundary conditions of automotive applications favor this failure mode strongly. Moreover, the use of other joining technologies than that used in the aircraft industry, such as joining by forming, leads to new challenges. The different influences, typical for joining by forming, on ultimate shear-out strength were first investigated separately and then transferred and validated on connections related to praxis by an analytical model. Special attention was given to effects that resulted from oversized pre-holes, acting clamping forces, and the reduced quality of the laminates in the immediate vicinity of the joint due to the joining process.

Keywords

CFRP, joining, strength, analytical modeling, defects

Introduction

Worldwide, legislations dictate that industries decrease the amounts of CO_2 emissions. In the European Union, the automotive industry, for example, stands confronted by a regulation, which stipulates that the average CO_2 emissions for new cars are to be reduced to 95 gCO_2/km until 2020, resulting in a decline of approximately 35% compared to 2010.[1] Next to engine optimizations, the development of lightweight structures is contributing to fulfilling the requirements of environmental legislations as well as the satisfaction of customer needs.[2] Beside the use of aluminum space frame structures or ultra-high strength steels, great effort is put forward in the development of multi-material body structures containing carbon fiber reinforced plastics (CFRP).[3]

Within the space and aircraft industry the use of CFRP in structural components has been well known for many years. Hence there is wide knowledge of necessary machining and joining technologies that meet the requirements of highest quality for the aircraft industry. Similarly, extensive knowledge is at hand about methods to predict the strength of the joints on this basis. The use of CFRP in the automotive large-scale production, however, differs fundamentally as allowable costs and cycle times are much lower than in the aircraft industry resulting in a complete change of boundary conditions. This leads not only to the use of different laminate structures and manufacturing processes but also to the need for different joining technologies.

Joining by forming based on mechanical fasteners such as self-piercing rivets or flow-drill screws frequently deployed in combination with adhesive bonding is a technology widely used in the automotive body shop for manufacturing aluminum–aluminum or aluminum–steel structures.[4] Good reviews regarding blind riveting (BR), flow-drill screwing (FDS) and self-piercing riveting (SPR) are given in literature.[5–7] An adaption of these techniques to structures containing CFRP and one or more metallic partners comes with new challenges.[8] Especially, the reduced quality of the laminates in the immediate vicinity of the joint due to the self-piercing or self-drilling process and due to the deformation energy necessary for the joint formation seems critical. More so as the effects

[1]Bayrische Motoren Werke AG, Dingolfing, Germany
[2]Professur für Fügetechnik und Montage, Technische Universität Dresden, Dresden, Germany

Corresponding author:
Maximilian Felix Wilhelm, Bayrische Motoren Werke AG, Landshuter Straße 56, D-84130 Dingolfing, Germany.
Email: maximilian.f.wilhelm@bmw.de

of the thereby induced delaminations and interfiber breakages, further on referred to as imperfections, on the joints are widely unknown.

Beside the difference in manufacturing technologies, the change in the boundary conditions between the aircraft and automotive industry includes changed constructions and reduced product life cycle times. Aircraft models, for example, are followed by their successor after more than 15 years, whereas cars are succeeded by a new model about every 6 years. This leads to significant shorter product development times and an increase in necessary joint designing and testing. Although in most cases joining by forming is to be combined with adhesive bonding, the understanding of the basic mechanical joint is vital for assessing the overall characteristics of the joint and the properties of the material.

In the aircraft industry, joints are normally designed for bearing failure. Hence, the knowledge on this failure mode is wide. Literature, for example, covers different stress analysis and strength prediction models, both analytical and numerical, as well as experimental investigations on bearing strength affecting parameters such as clamping force, stacking sequence or geometric boundary conditions.[9–15] Valuable pioneer work on the influence of the hole's quality on design bearing strength is also provided by Persson et al.[46] and Tagliaferri et al.[17] Although a significance of imperfections is stated, no detailed connection between the degree or the amount of imperfections and the resulting strength is drawn.

The changed constructive boundary conditions in the automotive industry lead especially to tendentially thinner and stronger anisotropic laminates as well as to restrictions in the available installation space which results in narrow flanges which all favor shear-out against bearing failure. Due to its undesired nature in the aircraft industry, research focusing on shear-out failure is scarce. However, existing research suggests that stress concentration is dependent on edge distance.[18–21] Especially, Lim et al.[18] state a strong dependency of the stress concentration factor on edge distance to hole diameter. Moreover, Wang et al.[14] state a positive influence on higher clamping forces on shearing strength complicating calculation further, although the effect is supposed to come from a higher friction force rather than the support of fibers against buckling through the lateral constraint as observed for bearing failure.

The aim of this paper is therefore to analyze different influences on the ultimate strength of connections joined by forming failing in shear-out mode. To eliminate interdependencies between the different influencing factors, the relevant parameters are first investigated separately. Subsequently, the different influences are put together in a mixed analytical–empirical model to evaluate the interdependencies for connections related to praxis. The relevant influences shall be addressed in the section ''Theory and calculation''.

Material and methods

In order to support a certain generality, experimental data were gained using the two deliberate diverse CFRP of Table 1. The first laminate is highly anisotropic and was manufactured from two layers of 50k triaxial-braided carbon/glass fiber hybrid material and an epoxy resin using resin transfer molding. The second laminate was manufactured from a more classic non-crimp fabric and a second epoxy resin by wet pressing. Both laminates have a fiber volume content of approximately 50% and represent composites currently in development for automotive applications at BMW. As shear strength is heavily dependent on testing procedure, the used standard DIN 53399-2:1982 shall be mentioned.[22] The properties of the Non-crimp material were not measured directly but calculated based on the characteristics of the UD-layers.

Quasi-static testing was conducted on a universal testing machine (Zwick XC-FR250SN) with a 250 kN load cell in displacement control at a rate of 10 mm/min.[23] Data regarding the individual influences, for example of imperfections, were gained by double-lap shear tests of specimens along the lines of DIN 65562:1991.[24] These specimens, as shown in Figure 1, have a hole of Ø5 mm and are joined by a finger-tightened bolt to avoid a resulting clamping force.

Data regarding the influences on connections related to praxis were gained by single-lap shear tests of two-point specimens joined by forming with the same main dimensions as those in Figure 1 and an edge distance $e = 10$ mm.[23] The specimens were manufactured using standard elements and equipment as given in Table 2 joining CFRP with a conventional steel of type CR240BH-GI50/50.[25]

The quality of the connections joined by forming was assessed by micro-sectioning and deemed in accordance to internal BMW quality standards. Figure 2 shows the micro-sections and gives an impression of the elements listed in Table 2.

Table 1. Mechanical properties of the composite laminates in 0° direction.

Material	Elastic modulus (GPa)	Shear strength R_{xy} (MPa)	Thickness t (mm)
Braided $(\pm 45^\circ G/0^\circ C)_s$	84	76	2.08
Non-crimp $(+45^\circ_{(1)}/-45^\circ_{(1)}/0^\circ_{(4)})_s$	62	176	1.90

As clamping force is known to play an important role regarding ultimate joint strength, knowledge of the acting clamping forces is vital in assessing the overall characteristics of the different connections. However, there is no state-of-the-art method for determining clamping force directly for each of the three joining techniques due to high process forces of up to 50 kN. To solve this problem, an indirect approach was developed in which the friction force ratio for each joining technique was directly measured using the braided material. Figure 3 shows the used method. It is based on pulling a thin steel sheet, with a recess cavity around the mechanical fastener, which is clamped between the original connection out of the double-lap in load control mode. To transfer the results to other materials of similar thickness, the coefficient of friction was determined in separate experiments with a clamping force of 5 kN.

To reproduce imperfections induced through joining by forming, a contact pressure is applied around the predrilled hole through a die with a diameter of 10 mm. This method seems more practical and in better agreement to the real inducement of imperfections by the joining processes as, for example, classic impact or punch shear tests considering the need for specific hole diameters. Appropriate contact pressures for both materials were chosen in pilot tests. For the braided CFRP a magnitude of 600 N/mm^2 and for the non-crimp CFRP a value of 800 N/mm^2 were selected. Preparation was conducted on a computer-controlled servomotor press of type Tox TZ-VSN 08.425461.A.001 in load control mode. For the

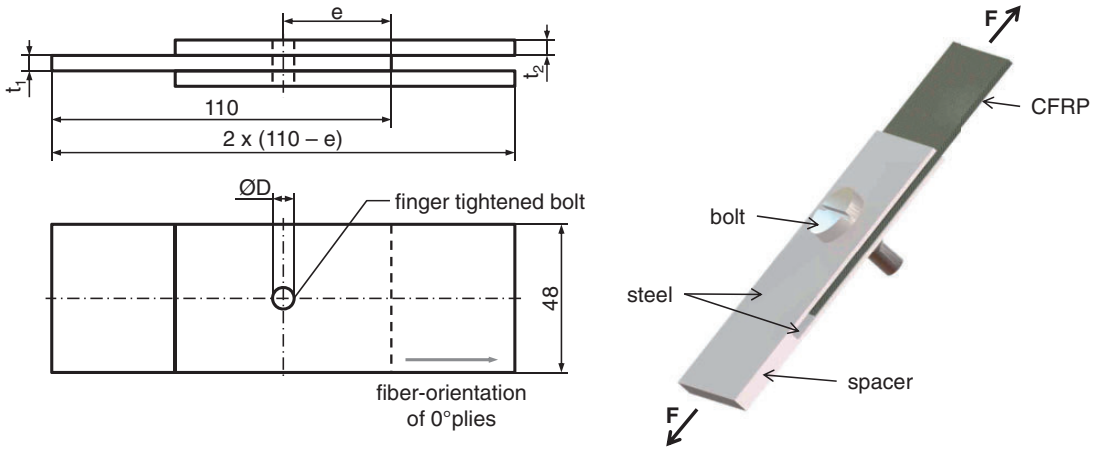

Figure 1. Specimen geometry joined by finger-tightened bolt for double-lap shear test.

Table 2. Elements and equipment used for manufacture of joints.

Technique	Element manufacturer	Element type	Ø-element, *D* (mm)	Joining equipment
Blind riveting (BR)	RIBE	wiredraw	4.8	Gesipa Taurus 2
Flow-drill screwing (FDS)	Arnold	flowform double tip	5.0	Weber RSF 20-2011
Self-piercing riveting (SPR)	Boellhoff	countersunk head	5.3	Tucker SRT 80 SXT

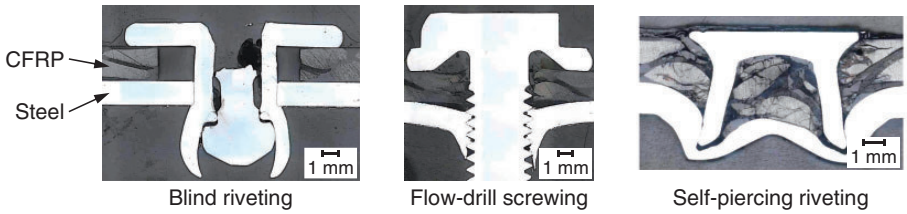

Figure 2. Micro-sections of connections joined by blind riveting, flow drill screwing and self-piercing riveting.

assessment of the induced imperfections ultrasonic testing in immersion technique was employed as other non-destructive testing methods fail for mechanical joints due to the high inhomogeneity of the multi-material connection including CFRP, steel and metallic joining elements.[26] The ultrasonic C-scans of the bottom echo were evaluated and areas with different degrees of attenuation of the incident pulse in the shear zone were measured.

Theory and calculation

The aim of the paper is to analyze different influences on the ultimate strength of connections joined by forming failing in shear-out mode. To do so, certain qualities and boundary conditions that are inherent to joining by forming or necessary for applications in the automotive body shop are implemented in the calculation of ultimate strength and evaluated. The basic equation for calculating the ultimate strength in shear-out mode F_{us} for composite materials and one mechanical fastener is given for example by Lim et al.[18] or Schuermann[27] as

$$F_{us} = 2et\hat{R}_{xy} \quad (1)$$

where $\hat{R}_{xy}$ is the shear strength of the notched laminate, e the edge distance and t the thickness of the specimen as defined in Figure 1. The following influences on ultimate strength shall be addressed resulting from a general lack of research focusing shear-out failure and the mentioned specifics of joining by forming:

1. In general, elastic behavior of the CFRP up to failure is not considered to affect edge distance. However, a certain reduction of edge distance and, therefore, of ultimate shear strength could occur due to the elastic deformation in the vicinity of the joint.
2. A constant cylindrical element shape is assumed in the equation but joining by forming often results in different geometric specifics.
3. No clamping force and, therefore, no load transmission by friction force is considered.
4. Due to highly automated production processes and tolerance chains, predrilled holes are heavily oversized rather than fitted perfectly to the element diameter resulting in changed edge distance ratios.
5. A reduction of ultimate shear strength as a consequence of imperfections due to joining by forming is not considered by the equation.
6. For bearing strength, a positive effect of lateral constraint and higher clamping forces is stated in literature due to stabilizing the laminate against the occurrence of delamination and micro-buckling. A similar behavior could be true for higher clamping forces acting against imperfections due to a closing of micro-rifts and, therefore, improving ultimate shear strength disproportionately stronger than expected due to an increase in friction force.

Influence of elastic behavior up to final failure

The mechanical stress of the joint leads to an elastic deformation of the CFRP specimen, thus, potentially resulting in a reduced edge distance. To evaluate the influence on ultimate shear strength the elastic deformation of the joint can be considered by using the slope c_{LL} of the linear zone in the load–displacement graph. The parameter c_{LL} can be determined by single-lap shear tests in combination with micro strain measurement. Based on the collected data, an equation can be

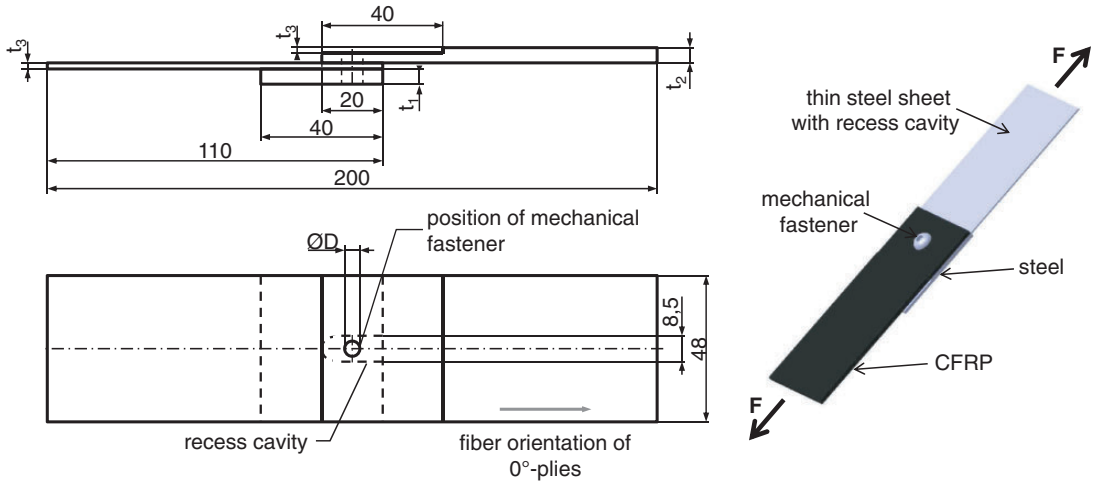

Figure 3. Specimen geometry joined by forming for measurement of friction ratio.

fitted to the linear zone of the load–displacement curve, using the method of least squares. The slope of this linear equation equals the parameter c_{LL} which can be interpreted as the stiffness of the joint. The elastic deformation y at a defined load F can be calculated with

$$y = \frac{F}{c_{LL}} \tag{2}$$

By subtracting the elastic deformation from the edge distance, its influence is considered leading to equation (3) for the calculation of the ultimate load in shear-out mode for a given elastic deformation y.

$$F_{us} = 2(e - y)t\hat{R}_{xy} \tag{3}$$

In order to calculate the ultimate shear-out strength in relation to the elastic deformation, equations (2) and (3) have to be combined and solved for F_{us} under fulfillment of the limit case $F = F_{us}$. The solution of the combined equations characterizes the ultimate strength F_{us} at which the bond fails under consideration of the elastic deformation.

Geometric specifics of mechanical fasteners

Equation (1) is valid for cylindrical element shapes as it assumes a straight shear plane by using laminate thickness t as the through-the-thickness crack length. Based on the geometric specifics of the self-piercing rivets as well as the flow-drill screws, especially the countersunk head, the spread rivet skirt and the screw threads, an elongation of the through thickness crack length could be presumed. Such an elongation would lead to an increase of shear plane and by that to an increase of ultimate shear strength for these joining techniques. To evaluate this effect, examinations of the sheared-out laminate pinch-offs and the shear planes were performed in pretests. For all joining techniques, a rather straight through-the-thickness shear plane could be observed so that calculation on the basis of a straight shear plane seems valid.

Calculation with clamping force

For bearing failure, an increase in ultimate bearing strength F_{ub} by load transfer through friction forces can be assumed leading to

$$F_{ub} = \hat{R}_b Dt + \mu_o F_c \tag{4}$$

where $\hat{R}_b$ is the bearing strength of the notched laminate, D the diameter of the joining element or bolt, μ_0 the coefficient of static friction, and F_c the axial clamping force.[27] An analogous correlation should be true for ultimate shear-out strength resulting in

$$F_{us} = 2et\hat{R}_{xy} + \mu_o F_c \tag{5}$$

Moreover, an increase in $\hat{R}_b$ for increasing clamping forces is stated in the literature for ultimate bearing strength but not for ultimate shear-out strength, so that equation (5) should yield even a better characterization for shear-out failure than equation (4) for bearing failure.[13,14]

Calculation with bolt/hole-clearance

Oversized predrilled holes lead to a bolt/hole-clearance that results in a load carrying through friction alone at the beginning of stressing the joint. When the static friction load is exceeded with raising stress level, as can be seen in Figure 4 at point I, the joint starts to slip in section II, and as a consequence of this slipping the edge distance is reduced. At the beginning of section III in Figure 4, the bolt contacts the edge of the predrilled hole and the load is carried by friction and tight fit, which shows in a sharp raise of load until the joint crashes in shear-out failure at point IV.

This reduction of edge distance e to a load-bearing edge distance e_b can be calculated by

$$e_b = e - 0.5\sqrt{d^2 - D^2} \tag{6}$$

as the intersection point of the circle equation of the predrilled hole and the tangent in the load direction on the bolt as shown in Figure 5.

For this calculation, it is assumed that the course of the shear plane is in line with the tangent from the bolt in the direction of the load. Under this assumption, $e_b = e$ for perfect bolt fit, so that, in the equations for ultimate shear strength, e can be replaced by e_b. For BR in the joining direction steel to CFRP, a perfect fit is assumed despite the element diameter of $D = 4.8$ mm and the hole diameter $d = 5.0$ mm due to the radial expanding which is characteristic for all wiredraw blind rivets.

Calculation with imperfections

The imperfections due to joining by forming are expected to reduce ultimate shear-out strength. As the degree of imperfections for each joining technique should be specific but relatively constant over varying edge distances, it is anticipated by the authors that a model that accounts for imperfections in a reduction of effective edge distances rather than to a reduced shear strength yields better results. Varying edge distance

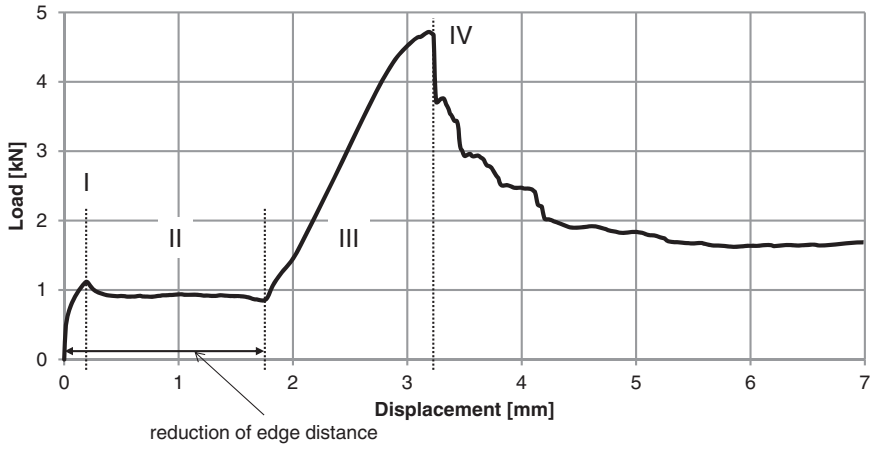

Figure 4. Exemplary load–displacement curve for a two-point blind riveted steel-CFRP connection with an oversized pre-hole in the steel partner.

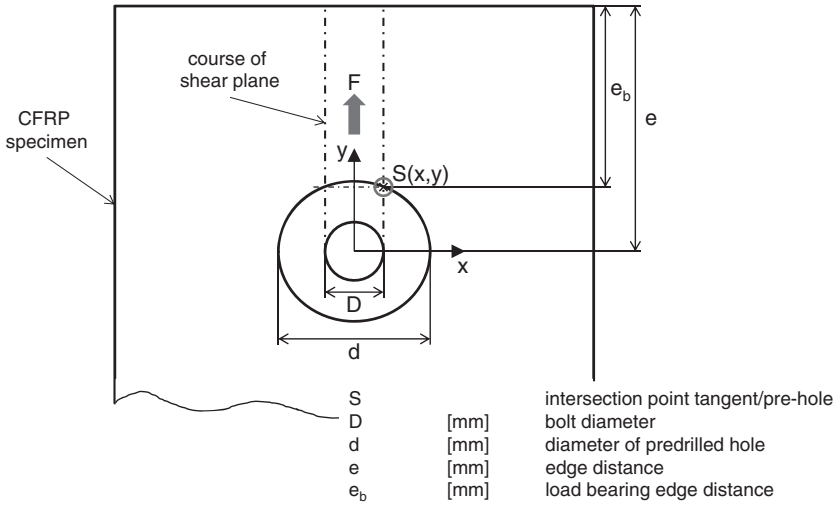

Figure 5. Reduction of load-bearing edge distance due to oversized pre-holes.

should lead to shifting ratios between areas uninfluenced and influenced by imperfections, thus, resulting in strongly declining shear strength values with declining edge distance undermining the possibility to calculate using a constant stress concentration factor or a constant notched shear strength. Different degrees of attenuation of the incident ultrasonic pulse can be interpreted as different degrees of imperfections at one particular point of the C-scan corresponding to one particular through-the-thickness line in the specimen. For each tested specimen, there is a pair of two shear planes which are shown in the C-scans by two lines as the upper and the lower shear planes. For these lines, the length of zones with different attenuation of incident pulse can be measured and can together be assigned to one shear-out strength. Figure 6 gives an example of the chosen measurement approach.

Appraisal shall be done analyzing the zones with 0–33% (blue hues), 34–66% (green and yellow hues) and 67–100% (red hues) attenuation of incident pulse leading to problem arrays of the form

$$\begin{matrix}\left(e_{\mathrm{u},1,i}\theta_{\mathrm{u},1,i}+e_{\mathrm{u},2,i}\theta_{\mathrm{u},2,i}+e_{\mathrm{u},3,i}\theta_{\mathrm{u},3,i}\right)=e_{\mathrm{u},i}\\ \left(e_{\mathrm{l},1,i}\theta_{\mathrm{l},1,i}+e_{\mathrm{l},2,i}\theta_{\mathrm{l},2,i}+e_{l,3,i}\theta_{\mathrm{l},3,i}\right)=e_{\mathrm{l},i}\end{matrix}\rightarrow F_{\mathrm{us},i} \quad (7)$$

with θ being the reduction ratio for edge distance due to imperfections, index i denoting sample number, index 'u' indicating the upper and 'l' indicating the lower shear line in the C-scan, index 1 denoting the zone

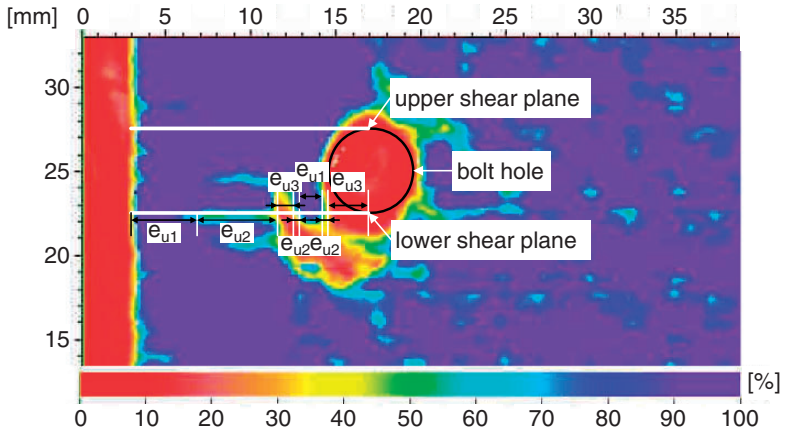

Figure 6. Measurement of zones with different degrees of attenuation in an ultrasonic C-scan.

with 0–33% attenuation, 2 denoting the zone with 34–66% attenuation and 3 denoting the zone with 67–100% attenuation. $F_{us,i}$ can further be modified by $F_{us}/(2t\hat{R}_{xy})$ to the effective edge distance $e_{eff,i}$ expected based on notched shear strength and laminate thickness leading to an objective relation of the form

$$e_{u,i} + e_{l,i} = 2e_{eff,i} \tag{8}$$

Based on this and the assumption that θ is equal for the upper and the lower shear line, the model function for a regression analysis can be written as

$$\begin{aligned}&(e_{u,1,i} + e_{l,1,i})\theta_{1,i} + (e_{u,2,i} + e_{l,2,i})\theta_{2,i} \\ &\quad + (e_{u,3,i} + e_{l,3,i})\theta_{3,i} = 2e_{eff,i} = \frac{F_{us,i}}{\hat{R}_{xy}t}\end{aligned} \tag{9}$$

and the overall optimization aim as

$$\min \sum_{i=1}^{n} (\theta_{1,i} - \theta_1)^2 + (\theta_{2,i} - \theta_2)^2 + (\theta_{3,i} - \theta_3)^2 \tag{10}$$

with n being the total sample size. It can be discussed that θ_1 should be chosen as an anchor value and fixed as $\theta_1 = 1$ indicating the full strength of the material. Next to the reduction ratios for the different attenuation levels, average values for the length of the attenuation zones for each joining technique have to be determined and taken into consideration. The load-bearing edge distance for joining by forming is then to be modified by the calculated values of θ_1–θ_3 and the specific $e_{u,1}$–$e_{l,3}$ for each joining technique in the following form to the effective edge distance

$$e_{eff} = \frac{\left[(e_{u,1} + e_{l,1})\theta_1 + (e_{u,2} + e_{l,2})\theta_2 + (e_{u,3} + e_{l,3})\theta_3\right]}{2} \tag{11}$$

In the absence of imperfections, it can be presumed that $e_{eff} = e_b$, so that in the equations for ultimate shear strength e as well as e_b can be replaced by e_{eff}. This step, however, leads to the deprivation of edge distance flexible calculation as the $e_{u,1}$–$e_{l,3}$ are edge distance specific. For the validation example in the "Results and discussion" section, an edge distance of 10 mm was chosen.[23] A certain portability of these values can be gained by increasing $e_{u,1}$ and $e_{l,1}$ analog to growing edge distance and decreasing $e_{u,1}$ and $e_{l,1}$ analog to shrinking edge distance assuming again a degree of imperfections that is specific to each joining technique but relatively constant over varying edge distances.

Results and discussion

Influence of elastic behavior up to final failure

The analysis of the single-lap shear tests with micro strain measurement, shown in Figure 7, shows an almost constant slope for all investigated joining technologies resulting in an elastic deformation that is rather independent of the joining technology used. The lowest slope could be observed for BR with $c_{LL} = 41.87$ kN/mm, thus, resulting in the strongest effect of elastic deformation among the investigated joining technologies. To eliminate the influence of oversized pre-holes, a perfect fit was used for both joining partners. Exemplary, the ultimate shear strength of a bolted connection without clamping force and imperfections was determined for the braided material using equation (3) to $F_{us} = 2.19$ kN instead of $F_{us} = 2.20$ kN based on equation (1). As the shortening of edge distance due to elastic deformation shows little effect on ultimate shear strength, but is experimentally elaborate to comprise, its influence shall be neglected further on to avoid an overloading of the aspired calculation model regarding complexity.

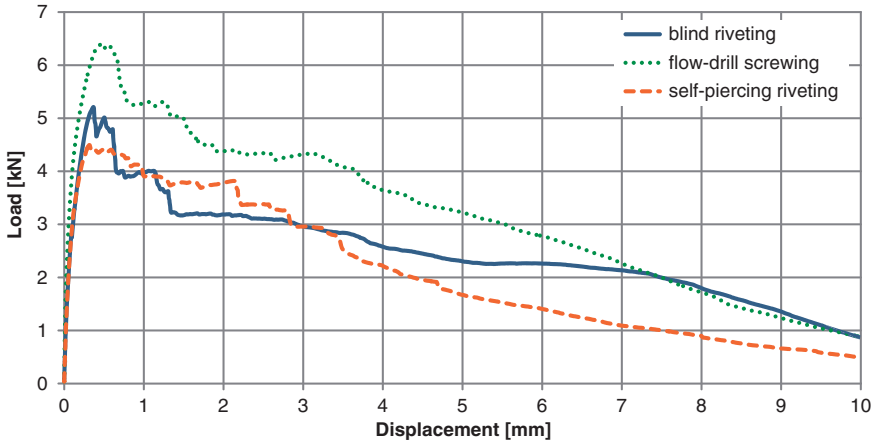

Figure 7. Micro strain measured load–displacement curves for determination of c_{LL}.

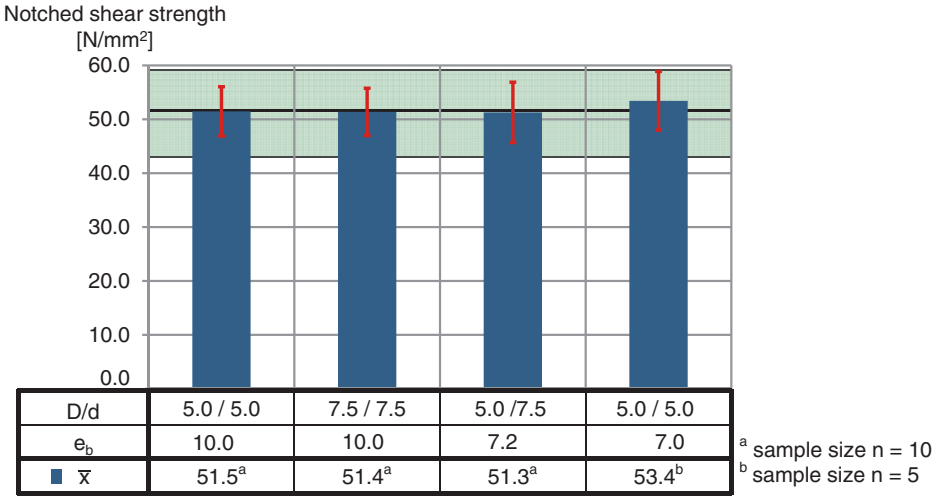

Figure 8. Effect of bolt diameter and bolt/hole-clearance on notched shear strength.

Calculation with bolt/hole-clearance

Experiments with the braided material and a sample size of $n = 10$, as in Figure 8, showed an independency for notched shear strength of bolt diameter and bolt/hole-clearance under the assumption of equation (6). On this basis the developed correlation for oversized pre-holes seems valid. Moreover, notched shear strength can be seen as constant in the relevant element diameter range.

Calculation with clamping force

The friction force ratios F_R, given in Table 3, were determined for the braided material using the developed approach with a sample size of 10. The friction coefficients for the used steel and each of the CFRPs were tested BMW internally and determined to $\mu_{0,\text{braided}} = 0.15$ for the braided and to $\mu_{0,\text{non-crimp}} = 0.13$ for the non-crimp material which is in accordance to values found in literature.[27] Based on this, the resulting clamping forces were calculated. To validate the data, a cross-check was done with friction force values gained of blind riveted one-point single lap specimens with an oversized pre-hole.[23] Analysis was done at point I, shown in Figure 4, of the load–displacement curves.

Moreover, clamping force was directly measured for FDS via load cell of type LORENZ-K1250 by Co. Arnold Umformtechnik in a two-step process. First, the hole and the thread in the steel sheet were formed by joining CFRP to steel by flow-drill-screwing and then removing the screw. Secondly, the load-cell was clamped between a predrilled CFRP and the prepared steel sheet with the tapped hole by a flow-drill screw tightened to 11 Nm, which equates to the torque of the

Table 3. Determination of clamping force for the different joining techniques.

Technique	Joining direction	$\bar{F}_R^b$ (measured) (kN)	F_c (calculated) (kN)	Cross-check (measured) (kN)
BR	CFRP in steel	0.26; $\sigma = 0.04$	1.69	$\bar{F}_R = 0.26^a$; $\sigma = 0.06$
BR	Steel in CFRP	0.37; $\sigma = 0.05$	2.45	$\bar{F}_R = 0.54^b$; $\sigma = 0.14$
FDS	CFRP in steel	0.79; $\sigma = 0.10$	5.25	$\bar{F}_c = 4.19^b$; $\sigma = 0.31$
SRP	CFRP in steel	0.44; $\sigma = 0.05$	2.94	–

[a]Sample size $n = 7$.
[b]Sample size $n = 10$.

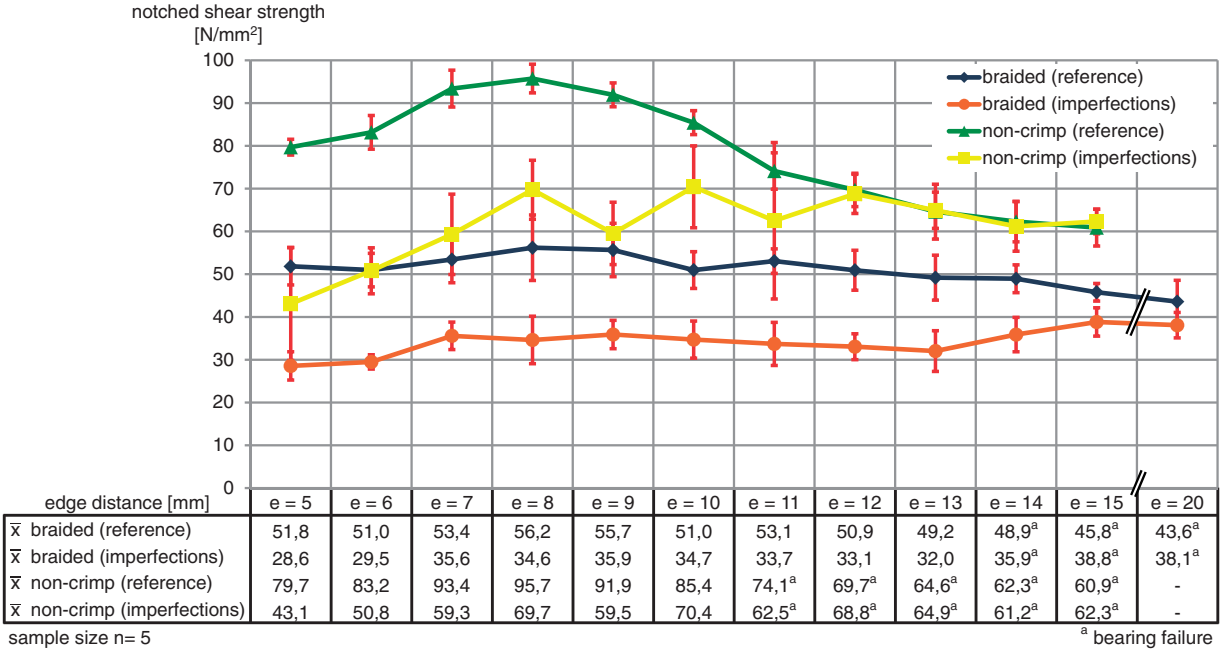

edge distance [mm]	e = 5	e = 6	e = 7	e = 8	e = 9	e = 10	e = 11	e = 12	e = 13	e = 14	e = 15	e = 20
x̄ braided (reference)	51,8	51,0	53,4	56,2	55,7	51,0	53,1	50,9	49,2	48,9[a]	45,8[a]	43,6[a]
x̄ braided (imperfections)	28,6	29,5	35,6	34,6	35,9	34,7	33,7	33,1	32,0	35,9[a]	38,8[a]	38,1[a]
x̄ non-crimp (reference)	79,7	83,2	93,4	95,7	91,9	85,4	74,1[a]	69,7[a]	64,6[a]	62,3[a]	60,9[a]	-
x̄ non-crimp (imperfections)	43,1	50,8	59,3	69,7	59,5	70,4	62,5[a]	68,8[a]	64,9[a]	61,2[a]	62,3[a]	-

sample size n= 5
[a] bearing failure

Figure 9. Notched shear strength of reference specimens and specimens with imperfections.

normal connections. The values for BR were in good agreement, which shows the general usability of the chosen approach. For FDS the directly measured clamping force was lower than the calculated one based on the measured friction force. This seems plausible as the steel is not plasticized in the second step leading to a higher friction coefficient which according to

$$F_c = \frac{M_A}{\frac{d_2}{2}\tan\left(\beta + \arctan\left(\frac{\mu_G}{\cos\left(\frac{\alpha}{2}\right)}\right)\right) + \mu_K \frac{D_K}{2}} \quad (12)$$

where M_A = torque, d_2 = diameter of thread flank, β = helix angle of thread, μ_G = coefficient of friction of the thread, α = flank angle, μ_K = coefficient of friction under screw head or nut, D_K = connecting surface of screw head or nut again leads to a lower clamping force by constant torque.

Calculation with imperfections

Double-lap shear tests under varying edge distances were performed with a sample size of 5 and are presented in Figure 9. Based on the ultimate shear strengths observed in the experiments, the notched shear strength for both materials was calculated. For edge distances for which specimens failed in bearing mode, shear strength was also calculated not as a true value but to support the general trend. Experiments showed a strong influence of imperfections on notched shear strength. For specimens tested with relatively large edge distances failing in bearing failure, first, a decrease, and then, almost no effect of imperfections was observed indicating that the damaged zone leads to a decrease in stiffness rather than to a decrease in ultimate strength. As ultimate strength, however, depends on the edge distance, and, therefore on stiffness for shear-out failure, an influence on ultimate strength is observed for specimens failing in this failure mode.

The slightly lower values for the braided material with imperfections compared to the reference are put into perspective by taking into account that due to the pressing process for reproducing imperfections a bolt of diameter $D = 4.80\,\text{mm}$ compared to a bolt of diameter $D = 4.95\,\text{mm}$ had to be used. As this does not influence ultimate shear strength, this characteristic comes into effect not before bearing failure becomes dominant.

For a better understanding of whether the effects of imperfections on through bolt connections can be transferred to connections joined by forming, their effect needs to be implemented in calculation. Based on the observations above, a calculation model which is built on a reduction of effective edge distance due to imperfections seems to be the right choice. For the experiments shown in Figure 9 and the corresponding measurement of imperfections the linear regression supplied the following reduction ratios for the braided material $\theta_1 = 0.92$, $\theta_2 = 0.64$ and $\theta_3 = 0.55$ as well as for the non-crimp material $\theta_1 = 1.00$, $\theta_2 = 0.99$ and $\theta_3 = 0.36$. The six sigma software tool Minitab 16 was used for the conducted regression analysis. In addition to the reduction ratios Minitab delivered a R^2-value, which provides an indication for the quality of matching between data and model, for the braided material of $R^2 = 98.93\%$ and for the non-crimp material of $R^2 = 98.03\%$ both values suggesting very good agreement. The mean error for the braided material was determined to be 1.45% and for the non-crimp material to be 6.82%. As mentioned, the factor θ_1 can be chosen as anchor value. Under this assumption the following factors were calculated for the braided material to be $\theta_1 = 1.00$, $\theta_2 = 0.62$ and $\theta_3 = 0.55$ and the mean error was determined to be 1.35%. As these results delivered again very good agreement and additionally a more satisfactory model from the technical point of view—as by this means the zones e_1 yield full material strength—this solution was chosen for further calculation. The non-crimp material delivered by default $\theta_1 = 1$, so no additional calculation was necessary. Additionally, the effective edge distances e_{eff} for both materials and all joining techniques were determined for an edge distance $e = 10\,\text{mm}$ and are shown in Table 5. Due to the relatively big screw head for FDS, the elements had to be removed before ultrasonic inspection.

Validation of the different influences on connections joined by forming

Based on the collected findings, the equation for calculating ultimate shear strength for connections joined by forming is written as

$$F_{\text{us}} = \left(2e_{\text{eff}} t \hat{R}_{\text{xy}} + \mu_{\text{o}} F_{\text{c}}\right) q \tag{13}$$

where q is the number of elements in parallel order. The separate investigations on the different influences were validated using this formula and ultimate strength values of the different joining technologies of standard specimens.[23] The mean values of 10 samples for $e_{\text{u},1} + e_{\text{l},1}$, $e_{\text{u},2} + e_{\text{l},2}$, and $e_{\text{u},3} + e_{\text{l},3}$ for the determination of e_{eff} are given for each joining technique in Table 4. For comparison, the joining technique independent values gained by multiplication of equation (1) with the number of elements shall be given for the braided material as 4.24 kN and 6.49 kN for the non-crimp material. For computation, $\hat{R}_{\text{xy, braided}} = 50.96\,\text{N/mm}^2$ and $\hat{R}_{\text{xy, non-crimp}} = 85.42\,\text{N/mm}^2$ were used as the shear strengths of the notched laminates at $e = 10\,\text{mm}$ as given in Figure 9.

Additionally, the values gained by equation (13) using e_{b} instead of e_{eff} are given in Table 5 to validate the approaches regarding clamping forces and oversized pre-holes under exclusion of the influence of imperfections. Table 5 shows the contrasting juxtapositions of calculation and experiment. Excellent agreement was found for the use of e_{b}, which indicates that clamping forces and oversized pre-holes have been considered correctly. Moreover, excellent agreement was found for the use of e_{eff} for BR in the joining direction CFRP in steel as in this case no imperfections have to be considered. For the other joining direction as well as the other two joining technologies, imperfections were considered as a reduced effective edge distance. An increased deviation between calculation and experiment can be observed for those cases with imperfections compared to those without. This negative deviation has to result from an interaction between clamping force and imperfections. Micromechanically, a closing of small cracks and, therefore, a support of the shear plane seems more likely than the subsidy against microbuckling which can be observed for bearing failure. Without considering imperfections at all, and by using e_{b} rather than e_{eff}, seemingly better agreement can be achieved. As, however, Figure 9 shows clearly

Table 4. Measured values for the joining technique specific $e_{\text{u},1}$–$e_{\text{l},3}$ for determination of e_{eff}.

Technique	Material	$e_{\text{u},1} + e_{\text{l},1}$ (mm)	$e_{\text{u},2} + e_{\text{l},2}$ (mm)	$e_{\text{u},3} + e_{\text{l},3}$ (mm)
BR	braided	9.10	4.86	6.03
	non-crimp	13.01	2.07	4.92
FDS	braided	1.89	5.54	12.57
	non-crimp	3.84	9.62	6.55
SRP	braided	4.45	5.35	10.20
	non-crimp	9.63	3.25	7.12

Table 5. Determination of ultimate shear strength for the different joining technologies.

Technique	Material	d (mm)	e_b (mm)	e_{eff} (mm)	F_{us} (calculated by e_b) (kN)	F_{us} (calculated by e_{eff}) (kN)	$\bar{F}_{us}$[a] (measured) (kN)	Error (equation (1)) (%)	Error (e_b) (%)	Error (e_{eff}) (%)
BR	braided	8.5	6.49	6.49	3.26	3.26	3.69; $\sigma = 0.33$	15	−12	−12
(CFRP in steel)	braided	5.0	10	9.30	4.45	4.45	4.92; $\sigma = 0.36$	−14	−9	−9
	non-crimp	8.5	6.49	6.49	4.67	4.67	4.94; $\sigma = 0.15$	31	−5	−5
BR	braided	5.0	10	7.72	4.98	4.01	4.83; $\sigma = 0.55$	−12	3	−17
(Steel in CFRP)	non-crimp	5.0	10	8.43	7.45	6.43	7.00; $\sigma = 0.25$	−7	6	−8
FDS	braided	–	10	6.12	5.82	4.18	5.57; $\sigma = 0.22$	−24	5	−25
(CFRP in steel)	non-crimp	–	10	7.87	7.91	6.52	7.96; $\sigma = 0.46$	−18	−1	−18
SPR	braided	–	10	6.69	5.13	3.72	4.56; $\sigma = 0.13$	−7	12	−18
(CFRP in steel)	non-crimp	–	10	7.72	7.28	5.80	7.33; $\sigma = 0.46$	−11	−1	−21

[a]Sample size $n = 5$.

Table 6. Determination of ultimate shear strength under consideration of an interaction between clamping force and imperfections.

Technique	Material	d (mm)	e_b (mm)	e_{eff} (mm)	F_{us} (calculated by e_b) (kN)	F_{us} (calculated by e_{eff}) (kN)	$\bar{F}_{us}$[a] (measured) (kN)	Error (e_b) (%)	Error (e_{eff}) (%)
BR	braided	5.0	10	8.20	4.98	4.21	4.83; $\sigma = 0.55$	3	−13
(Steel in CFRP)	non-crimp	5.0	10	9.09	7.45	6.86	7.00; $\sigma = 0.25$	6	−2
FDS	braided	–	10	6.57	5.82	4.37	5.57; $\sigma = 0.22$	5	−22
(CFRP in steel)	non-crimp	–	10	8.51	7.91	6.94	7.96; $\sigma = 0.46$	−1	−13
SPR	braided	–	10	7.97	5.13	4.26	4.56; $\sigma = 0.13$	12	−6
(CFRP in steel)	non-crimp	–	10	9.52	7.28	6.97	7.33; $\sigma = 0.46$	−1	−5

[a]Sample size $n = 5$.

the negative influence of imperfections, their effect has to be considered appropriately. To integrate the interaction of imperfections and clamping force further improvement of the developed model is necessary.

For FDS, a cross-check of the determined values was possible to an independent test series with the braided material in Wilhelm et al. with connections with varying pre-hole diameter.[28] For specimens with pre-hole diameter $d = 7$ mm and specimens with no pre-hole, equaling specimens with no imperfections but a reduction of load-bearing edge distance to $e_b = 7.45$ mm due to oversized pre-holes and specimens with imperfections but no reduction of load-bearing edge distance, the same ultimate shear strengths could be observed. Specimens with a pre-hole diameter $d = 5$ mm, equaling specimens with no imperfections and no reduction of load-bearing edge distance, showed an approximately 12% higher ultimate shear strength. This indicates that the induced imperfections equal a reduction of e_b of about 2.55 mm resulting in $e_{eff,FDS} = 7.45$ mm which indicates lower damage than the value of $e_{eff,FDS}$ gained by calculation based on Table 4 and equation (8) supporting the conjecture of an influence of clamping force on imperfections.

A correlation between clamping force and the thereby influenced square area with imperfections under the element head in the shear zone shall be assumed, in such a way, as the shear zone covered by the element head and, therefore, influenced by clamping force is assumed to yield full strength rather than the strength computed based on the reduction ratio. The shear zone covered by the element head can be calculated based on micro-sections of the connections or the measurement of the element head contour. The value was determined to be 1.05 mm for BR in the joining direction steel in CFRP, 1.00 mm for FDS and 2.83 mm for SPR. Under this assumption, excellent agreement between calculation and experiment is found as can be seen in Table 6. However, it is to be clarified that this step is a sole assumption, even though it is well founded and technically plausible.

Conclusions

An approach for measuring friction force and on this basis clamping force for connections joined by forming was developed and tested. Moreover, imperfections in the vicinity of the joint were found to influence strongly

the ultimate shear strength but not the ultimate bearing strength. A calculation model was developed that accounts for these influence factors as well as geometric boundary conditions such as oversized predrilled holes. A shortening of edge distance due to elastic deformation as well as specific geometries of the mechanical fasteners were judged of little relevance and are therefore not considered in the developed model. This seems valid as the calculated values using the model are in good agreement with experimental results. By comparing ultimate shear-out strength of the different joining technologies it is noticeable that connections by FDS deliver the highest ultimate strength despite the highest amount of imperfections due to their high friction force ratio. Based on the assumption of an interaction between clamping force and imperfections, the use of FDS-elements with a plane element head contact surface should yield even higher values than the used elements with the concave contour shown in Figure 2. This should be true as by the increased contact surface a bigger amount of imperfections would be equalized.

Funding

This work was supported by the Bayerische Motoren Werke Aktiengesellschaft.

Conflict of Interest

None declared.

Acknowledgements

One of the authors (Wilhelm M) wishes to thank BMW Group for funding this research as part of his Engineering Doctorate. The authors also wish to thank their colleagues at BMW Group and the company Arnold Umformtechnik who supported this work. They also thank Wilhelm A for proof reading, and Neugebauer M as well as Wagner J for discussion.

References

1. European Parliament. Regulation (EC) Nr. 443/2009—Setting emission performance standards for new passenger cars as part of the Communitýs integrated approach to reduce CO_2-emissions from light-duty vehicles. *Off J Eur Union* 2009; L 140: 1–15.
2. Fuessel U. Fügbarkeit—Systemlösungen bei Mischbauweisen. In: *9th Dresdner Leichtbausymposium 2005*, Dresden, Germany, 16–18 June 2005, paper no. 13, pp.13.1–13.14. Dresden: Selbstverlag der Technischen Universität Dresden.
3. BMW of North America LLC. BMW i3 Concept. The Megacity Vehicle. *Online Referencing,* http://www.bmw-i-usa.com/en_us/bmw-i3/ (2013, accessed 9 June 2013)
4. Barnes TA and Pashby IR. Joining techniques for aluminum space frames used in automobiles Part II—adhesive bonding and mechanical fasteners. *J Mater Process Technol* 2000; 99: 72–79.
5. Sadowski T, Knéc M and Golewski P. Experimental investigations and numerical modeling of steel adhesive joints reinforced by rivets. *Int J Adhes Adhes* 2010; 30: 338–346.
6. He X, Pearson I and Young K. Self-pierce riveting for sheet materials: State of the art. *J Mater Process Technol* 2008; 199: 27–36.
7. Birkelbach R. Fastening technique for hybrid auto body structures. In: *Fügen im* Karosseriebau 2012, Bad Nauheim, Germany, 17 April–19 April 2012, paper no. 2.17, pp. 1–40. Hannover: Vincentz Network.
8. Kroll L, Mueller S, Mauermann R, et al. Strength of self-piercing riveted joints for CFRP/aluminum sheets. In: *18th International Conference on Composite Materials*, Jeju Island, Korea, 22–26 August 2011, paper no. M16-4, pp. 1–6. Seoul: The Korean Society for Composite Materials.
9. Pisano AA and Fuschi P. Mechanically fastened joints in composite laminates: evaluation of load bearing capacity. *Compos Part B Eng* 2011; 42: 949–961.
10. Gray PJ and McCarthy CT. A global bolted joint model for finite element analysis of load distributions in multi-bolt composite joints. *Compos Part B Eng* 2010; 41: 317–325.
11. Thoppul S, Finegan J and Gibson RF. Mechanics of mechanically fastened joints in polymer-matrix composite structures—a review. *Compos Sci Technol* 2009; 69: 301–329.
12. Kelly G and Hallström S. Bearing strength of carbon fibre/epoxy laminates: effects of bolt-hole clearance. *Compos Part B Eng* 2004; 35: 331–343.
13. Park HJ. Effects of stacking sequence and clamping force on the bearing strengths of mechanically fastened joints in composite laminates. *Compos Struct* 2001; 53: 213–221.
14. Wang HS, Hung CL and Chang FK. Bearing failure of bolted composite joints. Part I: experimental characterization. *J Compos Mater* 1996; 30: 1284–1313.
15. Eriksson I. On the bearing strength of bolted graphite/epoxy laminates. *J Compos Mater* 1996; 24: 1246–1269.
16. Persson E, Eriksson I and Zackrisson L. Effects of hole machining defects on strength and fatigue life of composite laminates. *Compos Part A* 1997; 28: 141–151.
17. Tagliaferri V, Caprino G and Diterlizzi A. Effect of drilling parameters on the finish and mechanical properties of GFRP composites. *Int J Machine Tools Manuf* 1990; 30: 77–84.
18. Lim TS and Lee DG. Mechanically fastened composite side-door impact beams for passenger cars designed for shear-out failure modes. *Compos Struct* 2002; 56: 211–221.
19. Matthews FL. Experimentally determined strength of mechanically fastened joints. In: Matthews FL (ed.) *Joining in fibre-reinforced plastics*, 1st ed. Barking: Elsevier Applied Science Publishers, 1987, pp.65–104.
20. Hart-Smith LJ. Design and empirical analysis of bolted or riveted joints. In: Matthews FL (ed.) *Joining in fibre-reinforced plastics*, 1st ed. Barking: Elsevier Applied Science Publishers, 1987, pp.227–270.
21. Crews JH, Hong CS and Raju IS. *Stress-concentration factors for finite orthotropic laminates with a pin-loaded*

hole. Hampton: National Aeronautics and Space Administration, 1981. NASA Technical Paper 1862.
22. DIN 53399-2:1982. Testing of reinforced plastics; shear test on plane specimens.
23. BMW Group Standard 96012:2012. Joining Technology—shear testing and cross tension testing - specimen dimensions, tests. (Equivalent to ISO 14273:2000.).
24. DIN 65562:1991. Aerospace; fibre reinforced plastics; testing of multidirectional laminates; determination of bearing strength. (Equivalent to ASTM D5961/D5961M–13.).
25. VDA 239-100:2011. Sheet steel for forming.
26. Wilhelm M, Fuessel U, Nancke T, et al. Herausforderung CFK-Stahl-Mischbau: Quantifizierung von Delaminationen infolge des umformtechnischen Fügens. In: *Annual conference of the German society for non-destructive testing (DGZfP)*, Dresden, Germany, 6–8 May 2013, paper no. Mi.3.C.1-, pp. 1–10. Berlin: DGZfP.
27. Schuermann H. *Konstruieren mit Faser-Kunststoff-Verbunden*, 2nd ed. Berlin/Heidelberg: Springer, 2007.
28. Wilhelm M, Forster A, Fuessel U, et al. Umformtechnische Fügbarkeit von Faserkunststoffverbunden—Herausforderungen und optimierte Verfahrenslösungen: Das Fließformschrauben. In: *10th Dresdner Fügetechnisches Kolloquium*, Dresden, 23–24 May, 2013. pp. 136–142. Dresden: Selbstverlag der Technischen Universität Dresden.

Appendix

Notation

c_{LL}	slope of the load–displacement function in the linear zone (kN/mm)
d	hole diameter (mm)
D	element/bolt diameter (mm)
d_2	diameter of thread flank (mm)
D_K	connecting surface of screw head or nut (mm)
e	edge distance (mm)
e_b	load bearing edge distance due to oversized predrilled holes (mm)
e_{eff}	effective edge distance including a reduction due to imperfections (mm)
e_l	zone of a certain attenuation in the lower shear plane due to imperfections (mm)
e_u	zone of a certain attenuation in the upper shear plane due to imperfections (mm)
F	Load (kN)
F_c	axial clamping force (kN)
F_R	friction force (kN)
F_{ub}	ultimate strength in bearing mode (kN)
F_{us}	ultimate strength in shear-out mode (kN)
K	stress concentration factor (−)
M_A	Torque (Nm)
R^2	indication for the quality of matching between data and regression model (−)
R_{xy}	shear strength of the unnotched laminate (N/mm^2)
$\hat{R}_b$	bearing strength of the notched laminate (N/mm^2)
$\hat{R}_{xy}$	notched shear strength of the laminate (N/mm^2)
t	Thickness (mm)
y	elastic deformation (mm)
α	flank angle (°)
β	helix angle of thread (°)
θ	specific reduction ratio for edge distance due to imperfections of a certain attenuation (−)
μ_0	coefficient of static friction (−)
μ_G	coefficient of friction of the thread (−)
μ_K	coefficient of friction under screw head or nut (−)
σ	standard deviation (−)
$Ø$	Diameter (mm)

Indices

i	index for denoting the sample number
l	Index for denoting the lower shear line in the C-scan
u	Index for denoting the upper shear line in the C-scan
1	index for denoting the zone with 0–33% attenuation
2	index for denoting the zone with 34–66% attenuation
3	index for denoting the zone with 67–100% attenuation